行政院國家科學委員會補助專題研究計畫期中報告

X-ray 及電子束(e-beam)直接微影技術在多層導體連線上的應用研究(2/2)

Study on X-ray and E-beam Direct Patterning Technology for Multilevel Interconnect Applications

計畫編號：NSC　94－2215－E－009－011－
執行期間：94 年 08 月 01 日至 95 年 07 月 31 日

計畫主持人： 施敏 交通大學電子工程學系
計畫參與人員： 張大山 清華大學電子工程所
王敏全 清華大學材料所
楊富明 交通大學電子所

一、中文摘要

本計畫將針對 X-ray 及電子束(e-beam)曝光對低介電常數材料進行直接圖形化(direct patterning)技術進行研究：第一年，首先建立最佳的直接圖形化低介電常數材料的曝光參數。此外，銅金屬與經過 X-ray 及 e-beam 曝光後 Low-k 介電薄膜的交互作用也將在這一年內進行研究。在第二年，將運用此技術進行製程整合上的探討，包括 X-ray 及 e-beam 曝光及在顯影後所造成的介電特性穩定與否、抗熱能力、電性可靠度以及與銅金屬化學機械研磨相容性..等等。除此之外，我們也將利用 X-ray 與 e-beam 直接圖形化的技術製作銅導線的梳狀測試結構(comb structure)，並且進行共平面(in plane)介電特性、銅導線的電子遷移率可靠性之探討。此外，我們也將製作高頻測試結構進行載子高頻傳輸行為的研究。藉由以上所提的方式深入並廣泛地評估直接圖形化技術在 IC 製程應用上的可行性。

關鍵詞：低介電常數材料，X-ray，電子束，直接圖形化

Abstract

In this project, we propose X-ray and e-beam exposure to direct pattern the low-k dielectric in this study. In first year, we will establish the optimum exposure parameter for the direct patterning of low-k material. Moreover, we also study the interaction of Cu and low-k materials exposed by X-ray and e-beam. In second year, we will investigate the integration issues of this direct patterning technique on low-k material. This issue include the dielectric stability of low-k material after e-beam and X-ray exposure and development process, the thermal resistibility, electrical reliability, and the compatibility with copper CMP process etc.. In addition, we also make the Cu comb structure by this technique to do test. Simultaneously, we evaluate the dielectric properties of the inner layer of this structure and the reliability of electromigration for Cu interconnect. Furthermore, we also make high frequency test structure to investigate the carrier transfer

behavior under high frequency operation. Finally, we evaluate the feasibility of this technique during IC manufacture process.

Keywords: low-k dielectric, X-ray, e-beam, direct pattern

二、緣由與目的

As the complexity of function of the integrated circuit increases, the space between metal line and metal line become more narrow and longer. The phenomenon will cause the serious RC time delay, then reduce the operation speed of whole integrated circuit. In order to conquer the problem, the Cu metal and low k materials are utilized to replace the traditional Al metal and SiO_2 in semiconductor technology to enhance the IC performance. However, for defining device pattern in general IC manufacture process, we will utilize photoresist to define it. But the low-k dielectric will be degraded during the photoresist removal process. Furthermore, with the decrease of the structure size, the removal of PR is more and more difficult, resulting in the big challenge for pattern transfer step. To overcome this issue, we propose X-ray and e-beam exposure to direct pattern the low-k dielectric in this study. In addition, as the low-k dielectric is integrated with Cu, the dielectric properties will be demoted due to Cu diffusing into low-k materials.

三、實驗流程

The MSZ precursor solution diluted by its solvent propylene glycol monomethyl ether acetate (PGMEA) spin on Si wafer at 2000 rmp for 30 sec. After baking at 150 ℃ and 280 ^{o}C on a hot plate for 3 min, the films were transferred to a Leica Weprint200 stepper to carry out a curing process. The e-beam energy was 40 KeV with beam size of 20 nm. The doses of e-beam exposure were chosen with 100 to 800 uC/cm^2. Furthermore, the precursor solution of the porous organosilicate glass (POSG) diluted with MIBK were spun on Si wafers at the first-stage spin rate of 450 rpm for 4 s and the second 3000 rpm for 30 s, respectively. As-spun wafers were baked at 100 ^{o}C on a hot plate for 1 min. The resulting wafers were exposed blanketly by a Leica Weprint200 e-beam stepper with doses ranging from 2 uC/cm^2 to 820 uC /cm^2. The exposure doses of e-beam irradiation could be determined according to material and electrical analyses. As for the pattern formation of MSZ and POSG lines, as-baked MSZ and POSG films were irradiated with e-beam according to desire pattern layout. We observed the exposed pattern by scanning electron microscope (SEM) image to demonstrate the feasibility of e-beam direct patterning on MSZ and POSG films. The chemical structures of all aforementioned samples were characterized by Fourier transform infrared (FTIR Bio-Red QS300) spectroscopy. Electrical measurements were conducted on metal insulator semiconductor (MIS) capacitors. The dielectric constant measurements were conducted using a Keithley Model 82 CV meter. The area of the gate electrode was 0.00503 cm^2 for C-V analysis. The leakage current (I-V) characteristics were measured using a HP4156 electrical meter.

四、結果與討論

E-beam lithography process for the fabrication of damascene structure is shown in Figure 1. Figure 2 shows the leakage current of e-beam exposed MSZ film as compared to that of traditional furnace cured one. Unfortunately, the leakage current densities of e-beam exposed MSZ films are breakdown no matter what doses were applied. Moreover, the dielectric constant of e-beam exposed MSZ all can not be measured by C-V analyzer. Based on the results of electrical measurement, we deduce that the complete three-dimensional structure was not obtained by e-beam exposure. Therefore, there were many defects or leakage paths existed in the e-beam exposed MSZ films, which would cause the large leakage current. In order to enhance the dielectric properties of e-beam exposed MSZ films, we tried transferring these wafers to a furnace for further thermal annealing. Figure 3 shows the FTIR spectra of e-beam exposed MSZ with different doses after thermal annealing. The Si-OH groups of e-beam exposed MSZ film disappeared obviously after thermal annealing process. Furthermore, the functional groups of e-beam exposed MSZ films such as Si-O network-like peak, Si-CH_3 peak, and C-H peak etc. were all kept in high level the same as that of furnace-cured MSZ films. This indicates that the complete three-dimensional structure will be formed after thermal annealing for e-beam exposed MSZ films. The electrical properties of e-beam exposed MSZ film with different doses after thermal annealing is shown in Figure 4. The leakage current of all e-beam exposed MSZ films are improved to no more one order of magnitude than that of furnace-cured MSZ one. Nevertheless, the leakage current of e-beam exposed MSZ films increased with the increase of e-beam exposed doses. This possible reason is attributed to the defect generated from the e-beam exposure. The more doses is exposed, the more defect will be generated, which can not be recovered even after the thermal annealing process. On the other hand, the dielectric constants of e-beam exposed MSZ films are similar to furnace cured MSZ films after thermal annealing process. As a result, the clear pattern of single line of e-beam exposed MSZ film after development can be observed by optical image in Figure 5. Moreover, the cross section image of dense pattern lines of e-beam exposed MSZ film with 500 uC/ cm^2 after development is also shown in Figure 6. The dimension of the pattern line is about 120 nm.

Figure 7 reveals the leakage current densities of e-beam exposed POSG films at different doses with an additional annealing in a furnace at 400 ^oC for 30 min. It is clear that the leakage current densities are all significantly reduced after thermal annealing. Especial for the e-beam exposed sample with the dose of 8 uC/cm^2, its' leakage current density is recovered close to that of the furnace-cured one. The dielectric constant of e-beam exposed POSG films at different doses with thermal annealing is also shown in Figure 8. It is demonstrated that the dielectric constants of POSG films after e-beam exposure with thermal annealing in a furnace are decreased and close to the standard furnace-cured one. This indicate that even though the dielectric constants of POSG films after e-beam exposure are higher than that of the furnace-cured one, it can be recovered by additional thermal annealing process. Therefore, the results suggest that though available electrical dielectric properties of POSG film cannot be obtained directly by the e-beam curing process, the post-exposed thermal annealing process can be utilized to recover the electrical dielectric characteristics as the desirable pattern is formed by e-beam direct patterning process. In this study, we used a mixed solution containing 2.38 wt% tetramethylammonium hydroxide (TMAH) and methanol with the ratio of 1: 8 to develop the pattern, and the result is shown in Figure 9. Although the well contract of the pattern was not observed after development, it is clear that the e-beam direct patterning process can be achieved on POSG films. In addition, additional study is required to perfect the patterning resolution, but it is believed that this can be fine-tuned by varying the e-beam exposure dose and developed condition. In addition, after the development process of e-beam direct patterning for POSG films, an interesting phenomenon was found in the variation of dielectric characteristics of e-beam exposed POSG films. Therefore, we further investigated the possible mechanism by material and electrical analyses. Figure 10 presents the FTIR spectra of POSG films with e-beam exposure and followed by development and post-thermal annealing treatments. The FTIR spectra reveal that the functional groups (such as cage-like (~1144cm^{-1}) and network-like (~1049cm^{-1}) bonds of post-developed POSG films were weaker than that of as e-beam exposed POSG films. This implies that the uncrosslinked methyl-silsesquioxane matrix in films will be carried away by developer. Besides, the intensity of network-like peak was strong than that of cage-like peak in post-developed POSG film as compared to that of as e-beam exposed POSG film. This indicates that the e-beam exposure on as-baked POSG film only partially crosslink the methyl-silsesquioxane matrix into three-dimensional network structure. Once underwent the development process, the portion of uncrosslinked mono-polymer will be dissolved by developer used in this study. However, the crosslinked network structure of e-beam exposed POSG was carried away only a little during the development process. As a result, the network-like peak signal was stronger than the cage-like peak in the FTIR spectra of e-beam exposed POSG after development process. After subjected to thermal annealing at furnace, the residual uncrosslinked mono-polymer will be crosslinked and some remained developer solvent will be desorbed. Therefore, the intensity of network-like peak was larger than that of cage-like one after thermal annealing process. The above-mentioned reaction mechanism is illustrated in Figure 11. According to above analyses, we suggest that the porosity of e-beam exposed POSG film after development and thermal annealing processes will be higher than that as-cured POSG film. This mechanism can also be approved by electrical measurement. Figure 12 shows the leakage current density of e-beam exposed POSG films with 8 uC /cm^2 after underwent various treatments. The leakage current of e-beam exposed POSG film after development process was larger 2 to 3 order of magnitude than that of as e-beam exposed POSG films as measured at 1 MV /cm. Nevertheless, the leakage current of as developed POSG films can be recovered to that of as-cured POSG film through thermal annealing process. This implies that a number of leakage paths were generated during the development process due to that the portion of uncrosslinked material was carried away and replaced by the development solvent. After the thermal annealing process, the residual development solvent will be desorbed and the perfect network structure of POSG will be finished. Therefore, the leakage current of as-developed POSG can be recovered to similar to that of as-cured one after thermal annealing process. Figure 13 shows the dielectric constant of e-beam exposed POSG films with 8 uC /cm^2 dosage after underwent various treatment. It was found that the dielectric constants of POSG after e-beam exposure and development processes are all higher than that of as-cured POSG films. However, after underwent thermal annealing process, the dielectric constant was even lower than that of as-cured one to about 1.89.

五、計畫成果自評

We have performed e-beam lithography technique to direct pattern the low-k MSZ and POSG films. Materials analysis and electrical properties show e-beam exposure tends to give the as-hydrated MSZ energy to partial cross-linking the matrix material into three-dimensional structure. The sensitivity of e-beam exposure on MSZ film was about 500 uC /cm^2. Besides, the e-beam curing can provide POSG films energy to make the cage-like bonds of POSG partially transfer to network bonds. And the possible doses of e-beam exposure on POSG film is within the range of 8 uC /cm^2 to 16 uC /cm^2, which is satisfied the requirement of e-beam lithography technology. Such technique does not need the use of photoresist. It is believed that the technique can be incorporated into next generation of interconnect systems as the devices shrink into nano-scale regimes.

六、參考文獻

1. The National Technology Roadmap for Semiconductors, Semiconductor Industry Association, San Jose, CA (1997).
2. A. T. Kohl, R. Mimna, R. Shick, L. Rhodes, Z. L. Wang, P. A. Kohl, Electrochem. Solid-State Lett., **2,** 77 (1999).
3. A. M. Padovani, L. Rhodes, L. Riester, G. Lohman, B. Tsuie, J. Conner, S. Allen, P. A. Kohl, Electrochem. Solid-State Lett., **4,** F25 (2001).
4. T. Furusawa, D. Ryuzaki, R. Yoneyama, Y. Homma, K. Hinode, *J.Electrochem.Soc.,* 148, F175 (2001).
5. D. Thomas, G. Smith, and L. Nguyen, Int. Dielectrics for ULSI Multilevel Interconnection Conf. (DUMIC), 1997, pp. 361.
6. H. Meynen, R. Uttecht, T. Gao, M. V. Hove, S. Vanhaelemeersch, and K. Maex, in *Low and High Dielectric Constant Materials,* PV 98-3, 1998, pp. 29.
7. P. T. Liu, T. C. Chang, S. M. Sze, F. M. Pan, Y. J. Mei, W. F. Wu, M. S. Tsai, B. T. Dai, C. Y. Chang, F. Y. Shin, and H. D. Hung, Thin Solid Films, vol. 332, pp.345, 1998.
8. H. Namatsu, J. Vac. Sci. Technol. B, vol. 19, pp. 2709, 2001.

七、圖表

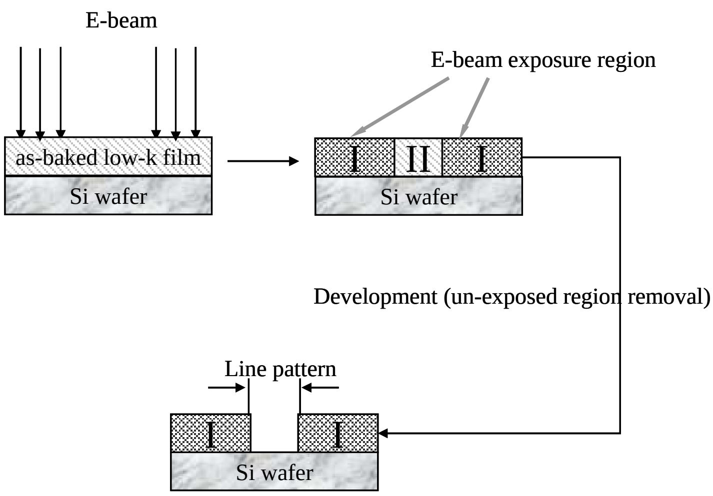

Figure 1 Proposed e-beam lithography process for the fabrication of damascene structure.

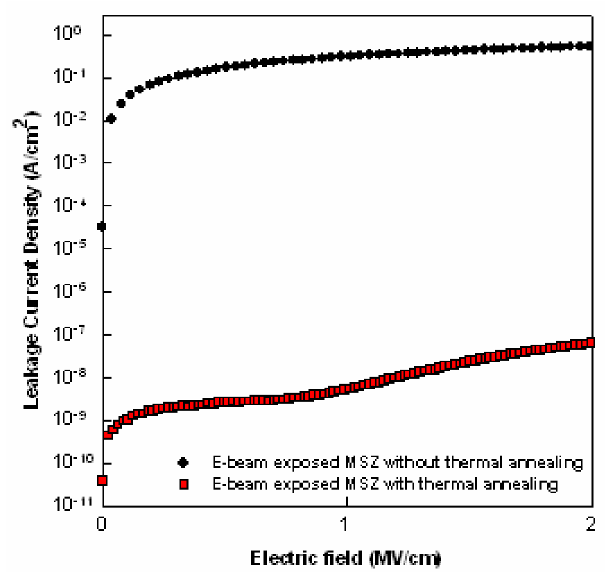

Figure 2 The leakage current of e-beam exposed MSZ is compared to that of traditional furnace cured one.

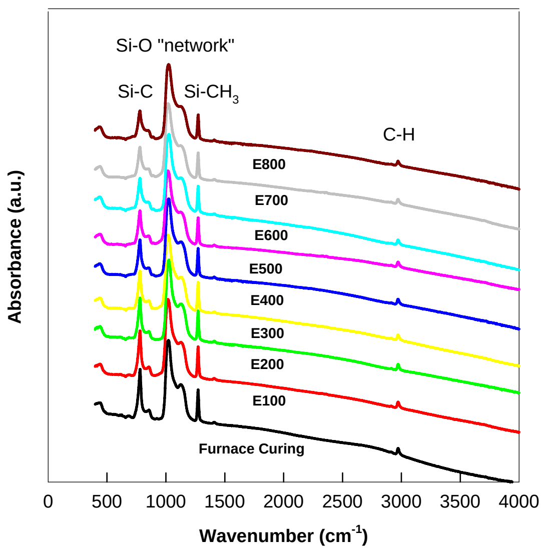

Figure 3 The FTIR spectra of e-beam exposed MSZ with different doses after thermal annealing.

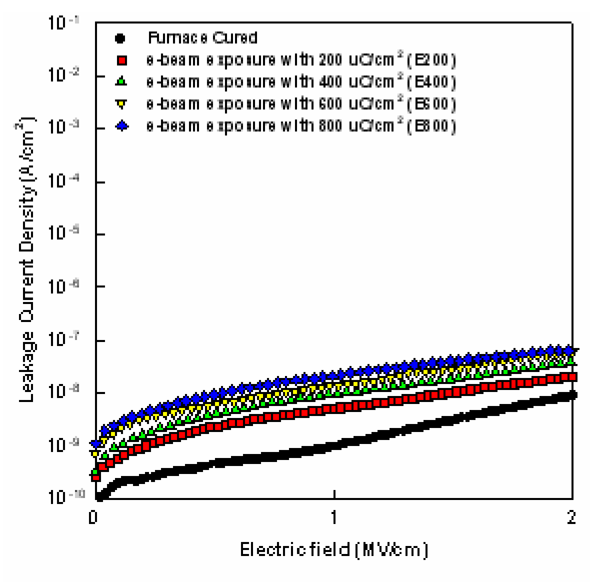

(a)

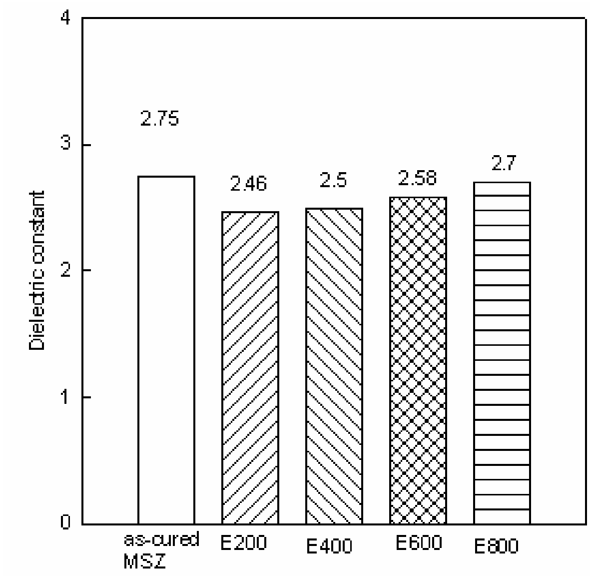

(b)

Figure 4 Dielectric properties of e-beam exposed MSZ with different doses after thermal annealing (a) leakage current density of MSZ films versus electric field (b) variation in dielectric constant of MSZ films

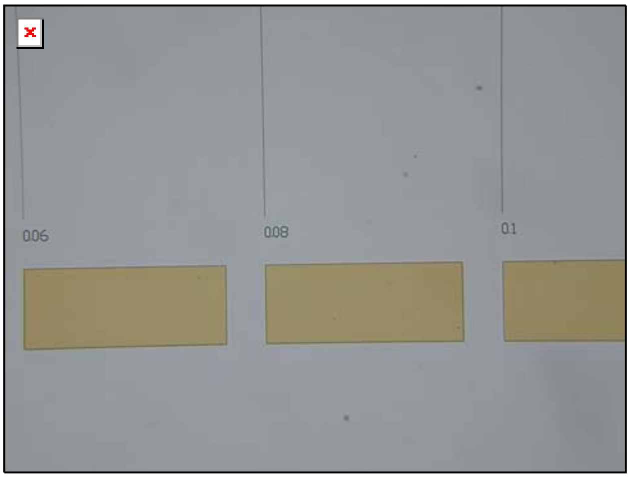

Figure 5 The optical image of single line pattern of e-beam exposed MSZ film after development.

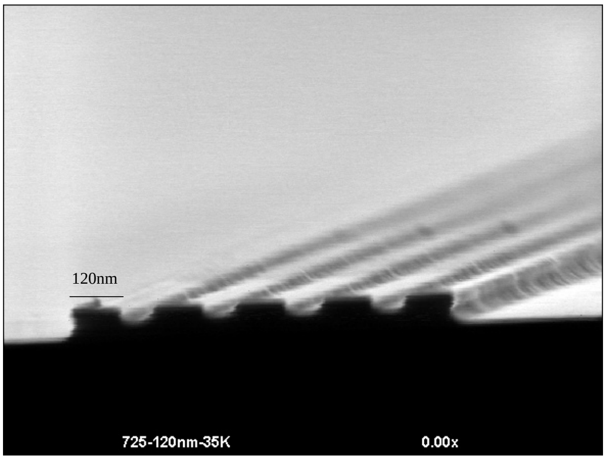

Figure 6 The SEM cross section image of dense pattern lines of e-beam exposed MSZ film after development.

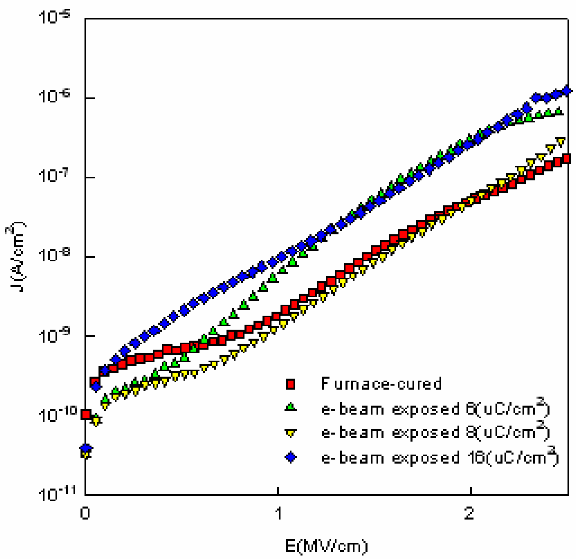

Figure 7 The leakage current densities of e-beam exposed POSG films at different doses. with furnace annealing process.

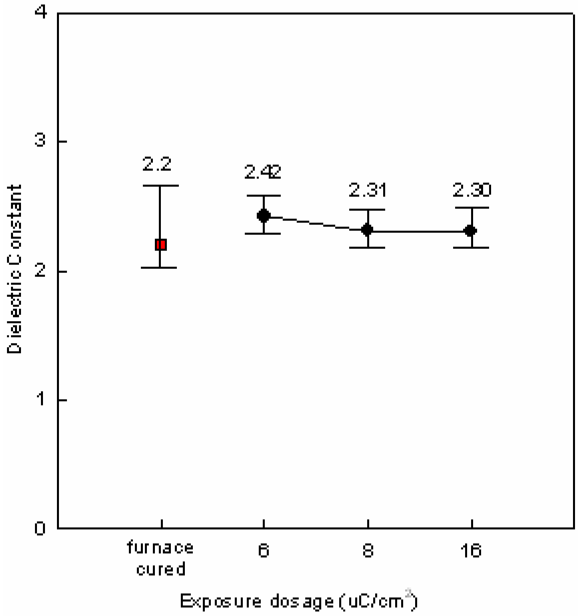

Figure 8 The dielectric constant of e-beam exposed POSG films at different doses with furnace annealing process.

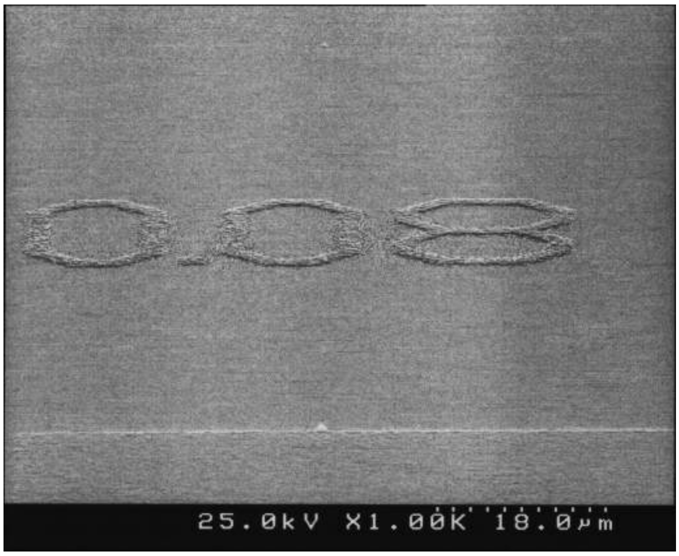

Figure 9 The SEM image of patterned wafer after e-beam curing and development processes without post-exposure annealing.

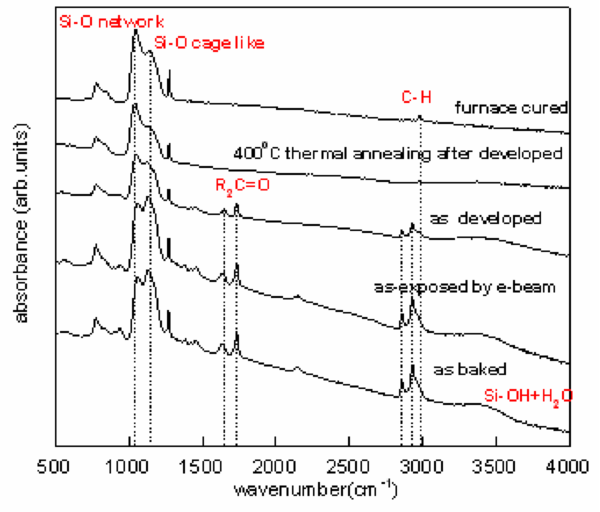

Figure 10 The FTIR spectra of POSG films with e-beam exposure and followed by development and post-thermal annealing treatments.

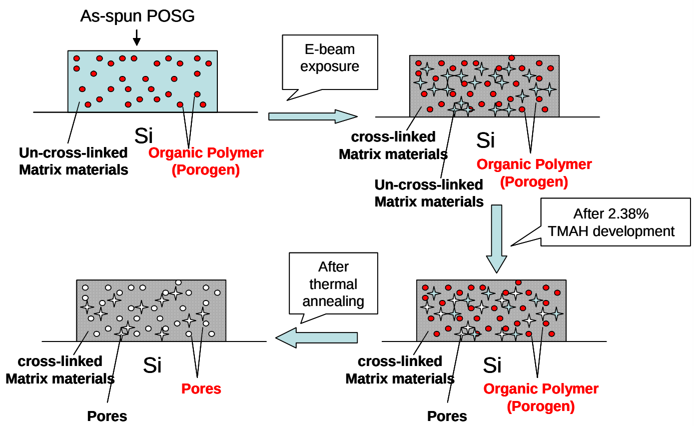

(a)

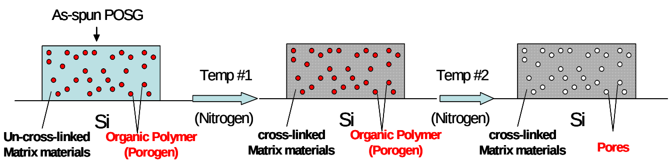

(b)

Figure 11 The proposed model for the decrease of dielectric constant on the e-beam exposed POSG after development and subsequent thermal annealing processes (a) e-beam direct pattering process (b) traditional furnace curing process.

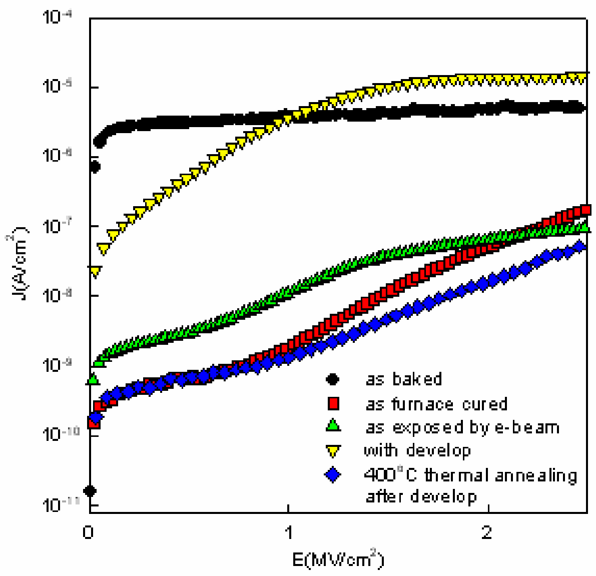

Figure 12 The leakage current density of e-beam exposed POSG films with 8 uC/cm^2 dosage after undergoing various treatment.

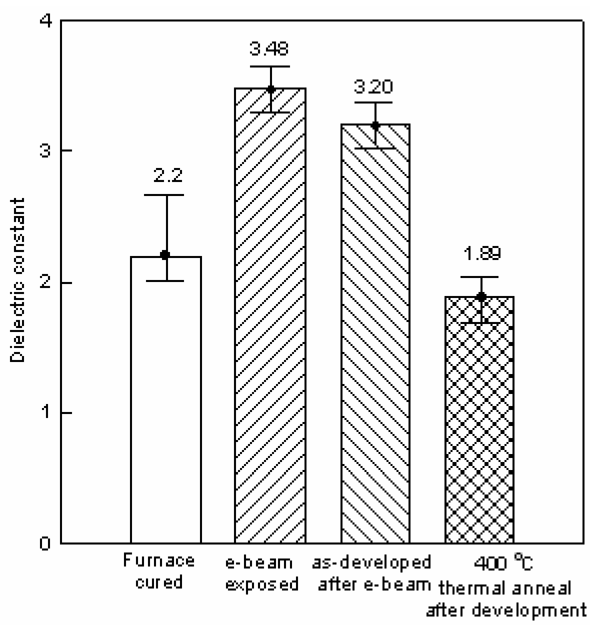

Figure 13 The dielectric constant of e-beam exposed POSG films with 8 uC/cm^2 dosage after undergoing various treatment.